JOURNAL OF MECHANICAL ENGINEERING AND SCIENCES
ISSN: 2289-4659 e-ISSN: 2231-8380
VOLUME 17, ISSUE 3, 2023, 9552 – 9563
DOI: https://doi.org/10.15282/jmes.17.3.2023.2.0756

RESEARCH ARTICLE

Detailed performance analysis of parabolic trough collectors including geometric effect

M. M. Kasem

Aerospace Engineering Department, Cairo University, Giza 12613, Egypt
School of Engineering and Applied Science, Nile University, Shaikh Zayed City 12588, Egypt

ABSTRACT - Parabolic trough collectors (PTCs) have been known for years as one of the leading methods for extracting energy from the sun. In the present work, the performance of PTCs was investigated. However, its performance needs some improvement to be integrated in more and wide range of applications. This idea motivated the author to investigate the performance of parabolic trough collectors in detail. Thus, in the present work, the performance of parabolic trough collectors is investigated. The effect of eight geometric and inlet variables on the PTC performance was evaluated. Two performance factors (PFs), the temperature difference and thermal efficiency, were selected. The effect of inlet condition, including inlet mass flow rate and inlet flow temperature reflector geometry, including reflector length and width,receiver diameters, including inlet and outlet reciever diameters, and cover diameters, including the inlet and outlet cover diameters on these PFs was assessed. Eight thermal working fluids were considered. A non-linear mathematical model was developed for PTC and implemented into MATLAB code where an iterative technique was used to conduct the present analyses. Level curves were generated to study the PTC key performance parameters. The curves revealed that the maximum values of the PFs and maximum range of change in these PFs occurred when the inlet conditions were varied. Changes in the inlet temperature, and changes in the reflector geometry yielded the highest and second-highest values. The cover geometry had the minimum effect on the PFs. Moreover, the best maximum efficiency, best maximum temperature difference, and maximum range of efficiency change were obtained for water, air, and carbon dioxide, respectively. The effect of inlet temperature is more significant than the mass flow rate effect on the thermal efficiency, whereas this effect is reversed in case of the temperature difference, by which the mass flow rate exerts the least influence on the temperature difference.

ARTICLE HISTORY

Received	:	21st Apr. 2022
Revised	:	15th July 2023
Accepted	:	21st Aug. 2023
Published	:	28th Sept. 2023

KEYWORDS

Parabolic trough collector
Thermal fluid
Performance analysis
Geometric effect
Inlet condition effect
Level curves

1.0 INTRODUCTION

Parabolic trough collectors (PTCs) are considered among the best sources of clear solar power [1]. The increase in the usage of PTCs stems from their high thermal efficiency and the demand for solar power as an alternative to the conventional energy sources [2]. The PTC technology was developed in the 1970s for heat applications and was introduced to the market in the 1980s [3]. Subsequently, PTC has become an important clear energy source for power generation. PTCs are fabricated from a bent sheet of reflected material, which is referred to as a reflector. The reflector usually has a parabolic shape for collecting and reflecting the solar irradiation onto a focal point at which a receiver tube is kept fixed. This tube is a metallic tube that is surrounded by a glass cover to reduce heat losses. A thermal working fluid moves through the tube, and the solar power increases the temperature and subsequently the thermal energy of the fluid [4]. The typical components and construction of a PTC are shown in Figure 1.

There are several types of PTCs available in literature based on its configuration and method of working. These types can be simpliy claaified into four main categories. First, the convensional parabolic trough collectors by which the collector takes a shape of a parabola. Second, the central reciver or flat collector in which the reflectors are flat. Third, the linear fresnel reflector which is built in linear arranbgement. Finally, the parabolic dish at which the reflector is formed as a dish [5]. PTCs have been extensively investigated because they can be implemented in several applications. PTCs can be used in water desalination to reduce salinity [6] and can also be utilized for power generation [7]. Hydraulic energy storage systems, such as hydraulic bladder-type accumulators, can be used along with PTCs for continuity in energy generation. These accumulators work as a backup system in PTCs [7]. Haghghi et al. [8] applied PTC technology in summer air conditioning. They integrated a PTC system with absorption chillers and an organic Rankine cycle for heating and cooling applications considering real solar radiation and energy load. The use of three-phase accumulator and solar absorption refrigeration along with PTC systems can maximize the PTC energy storage and ensure steady supply of cooling energy to buildings [9]. Ktistis et al. [10] evaluated the performance of a 288 m^2 PTC system used in industrial application for producing hot water and steam. The investigation lasted for two months and the effect of two operation

*CORRESPONDING AUTHOR | M. M. Kasem| ✉ mohamed.kasem@cu.edu.eg

strategies on the produced PTC amount of steam was assessed. They found that the PTC system can provide the required amount of steam even in the case of low solar radiation.

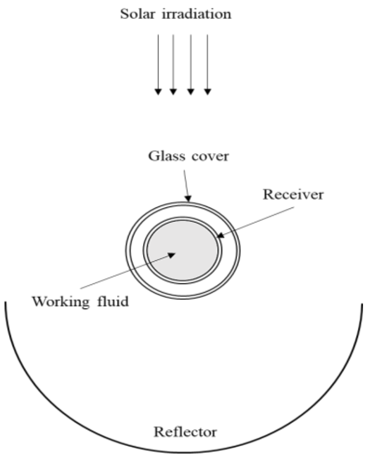

Figure 1. Components of PTC

Several mathematical and experimental models have been developed for the analysis, modeling, design, and testing of PTCs. The mathematical models are usually classified as optical analysis, thermal analysis, and heat transfer analysis [11] methods. Optical analyses can be considered the most important methods in PTCs, because the input of the thermal and heat transfer analyses usually depends on the output of the optical perfromance which in turn depends on the absorber surface flux distribution [3]. The PTC optical performance is also affected by the incident angle, effective sun shape, and optical errors (such as tracking error, slope error, and absorber alignment error) [12]. The optical analysis yields the optical efficiency, which is needed for the subsequent thermal and heat transfer analyses.

Thermal analysis usually focuses on obtaining the fluid temperature and the thermal efficiency of PTCs [11].Several thermal models have been developed for studying PTC thermal performance. Kalogirou [13] developed a detailed thermal model for the performance analysis of PTCs. In his model, he studied several modes of heat transfer including convection, conduction, and radiation. His model was used for the performance analysis of the PTC associated with the Cyprus University of Technology. Fasquelle et al. [14] developed a dynamic thermal model for PTC performance analysis aimed at simulating an unstable environment. The model was applied in two periods with different inlet conditions. The model was validated and was able to account for high input variations. In another study, the presence of metal foam and nano-fluids, along with water was quit efficient in improving the thermal performance of PTC and increasing the corresponding thermal efficiency [15]. The addition of metal foam can increase the friction factor by up to 80% compared with that obtained with water only. Lei et al. [16] developed computational fluid dynamic and finite element models for the thermal and stress analyses of PTC. They investigated the thermal and stress performance of PTC using numerical and experimental models. The results revealed that reducing the flow velocity, and inlet temperature and increasing the direct normal irradiation (DNI) can increase the temperature gradient and thermal stresses in PTCs [16].

Heat transfer analysis focusses on the performance of a heat collector element (HCE–the receiver tube) [11]. Padilla et al. [17] developed a one-dimensional numerical model for detailed heat transfer analysis of the HCE. They validated their model by comparing the obtained results with experimental results. The model can determine the collector efficiency and heat losses under different operating and flow conditions. They concluded that the heat transfer model performance can be significantly enhanced by reducing the convection heat losses. Jin et al. [18] established another method for evaluating PTC thermal performance using dimensional analysis and the similarity principle. Their model was calibrated using experiments and was then utilized to assess the effect of DNI and the temperature differences between the receiver and ambient temperature. The results revealed that the collector efficiency increased with increasing the DNI and decreased with decreasing temperature difference.

Zou et al. [19] developed an analytical model for finding the PTC intercept factor and the critical tube diameter including the effect of tube alignment error. Their model focused on the variation in optical performance including the effect of structural variables on optical efficiency. They found that (in contrast to results reported in previous work) the efficiency decreased with increasing offset angle. Salazar et al. [20] developed an analytical model for analyzing the performance of PTC power plants. The developed model simplified the evaluation of PTC performance, provided insight into the effect of PTC variables on system components, and explained the major trends exhibited by the system. Liang et al. [21] used analytical one-dimensional (1-D) and three-dimensional (3-D) models for the analysis of PTCs. When compared with experiments, the 1-D model was found to be more accurate than the 3-D model. The results revealed that 3-D models usually involve some numerical approximations. Fan et al. [22] developed a novel PTC model with dual glass tubes and thermal fluids. This model was found to be promising for cases involving inlet temperatures is lower than 150^{o}C.

Many variables can affect the performance of PTCs. Yadav et al. [23] investigated the effect of the reflector material on PTC performance. They observed that aluminum reflectors yielded better performance than steel reflectors. The use of the aluminum reflectors increased the maximum temperature by 24.2% and the thermal efficiency by 61.8 % compared with the use of steel reflectors. In another study, GO/water and AL_2O_3/water nano-fluids were compared in terms of thermal performance [24]; the GO/water-based nano-fluid exhibited better thermal performance than the AL_2O_3/water-based fluid. The operational effectiveness of nano-fluids especially in the presence of $AL_2O_{3,}$ decreased with increasing mass flow rate. Cheng et al. [25] studied the effect of aperture width on the PTC optical performance and found that the PTC sensitivity to optical errors increased with increasing the aperture width. Yuanjing et al. [26] developed an optimization model for improving the efficiency of a 30 MW PTC power plant. The developed model increased the overall efficiency of the plant by 0.22 % enhanced its thermal efficiency by 0.52 % and led to reduction in the total number of collectors needed in the power plant.

Padilla et al. [27] evaluated the effect of operational and environmental factors on PTC performance. They assessed the effect of mass flow rate, inlet temperature, wind speed, solar irradiation, and PTC tube outer pressure on PTC thermal and exergetic performance. The results revealed a significant effect of the irradiation, temperature, and pressure on the performance. However, the mass flow rate and wind speed had negligible effect on the performance. The use of a double glass envelop in PTCs has led to a reduction in heat losses and better performance than that of conventional PTCs [28]. Kumaresan et al. investigated (via experiments) PTC performance during a day in India. The results revealed that the best useful heat gain and incident beam radiation occurred between 8:00 and 9:00 am. The peak PTC efficiency occurred at 12:00 pm. After 14:00 the heat loss exceeded the heat gain. When comparing between the PTC losses, the absorber tube convection loss was found to have the major effect [29]. Yang et al [30] developed a novel receiver design with superior performance that is much better than the traditional receivers. Kasem [31] developed a novel design optimization model for the analysis and design of PTCs that was found to be efficient in enhancing PTCs performance by increasing the thermal and exergetic effeciencies. Most of previous studies concentrated with selected working fluids and performance parameters. Thus, in the present work, the author conducted a detailed study of eight working fluids including environment conditions, inlet conditions, and different geometric parameters.

The present study conducts a detailed performance analysis of PTCs using level curves (surface plots) to determine the effect of geometric and inlet flow conditions on their performance. Eight working fluids (water, Therminol, molten salt, liquid sodium, air, carbon dioxide, helium, and hydrogen) are considered in the present analyses. These fluids represent four liquids and four gases that are typically used in PTCs. The effects of inlet condition, reflector geometry, receiver geometry, and cover geometry on the PTC PFs (i.e. the PTC temperature difference and thermal efficiency) are investigated. A PTC non-linear mathematical model is implemented using a MATLAB code to generate thirty-two level curves for the eight thermal fluids used in the present study.

2.0 PTC MATHEMATICAL MODELING

PTCs harvest the sun energy and transform this energy into a thermal energy applied to a working fluid. This thermal energy can be used directly or extracted as a form of electric power that can be used in several applications. As shown in Figure 1, a thermal working fluid moves in a central tube (referred to as a receiver), which is surrounded by a glass cover. The tube and cover are placed in the focal point of a reflector that reflects the sunlight into the focal point and subsequently heats the working fluid. The amount of solar energy available is determined from [2].

$$\boldsymbol{Q_s = A_a\ G_b} \tag{1}$$

A thermal fluid can only capture some of the energy available. We define the energy that can be captured as the amount of energy that can be extracted by the working fluid. This energy can be determined as follows,

$$\boldsymbol{Q_u = m^o\ C_p\ (T_{out} - T_{in})} \tag{2}$$

Heat losses of the PTCs can lead to a decrease in the amount of energy attainable. These heat losses can be determined as follows,

$$\boldsymbol{Q_{loss} = A_{co}\, h_{out}\left(T_c - T_{amp}\right) + A_{co}\, \sigma\, \epsilon_c\, \left(T_c^4 - T_{amp}^4\right)} \tag{3}$$

The relation between the total available energy, useful energy, and energy losses can be determined from the balance equation [2]

$$\boldsymbol{Q_u = Q_s\, \eta_{opt} - Q_{loss}} \tag{4}$$

The useful energy is related to the receiver temperature follows,

$$\boldsymbol{Q_u = h\ A_{ri}\left(T_r - T_{fm}\right)} \tag{5}$$

Two PFs are considered in the present analyses: the thermal efficiency (η_{th}) and the temperature difference (ΔT), where

$$\boldsymbol{\eta_{th} = \frac{Q_u}{Q_s}\,,\ \Delta T = T_{out} - T_{in}} \tag{6}$$

The PTC cover and receiver areas as well as flow constants, used in the previous equations, are listed in Table 1. This non-linear model of PTC is implemented into a MATLAB code where an iterative technique for performing the present performance analyses is employed.

Table 1. PTC geometric areas and flow constants

Geometric areas		Flow constants	
$\boldsymbol{A_{co}}$	$\pi D_{co} L$	Re	$\frac{4m^o}{\pi\ D_{ri}\mu}$
$\boldsymbol{A_{ro}}$	$\pi D_{ro} L$	Pr	$\frac{\mu C_p}{k}$
$\boldsymbol{A_{ci}}$	$\pi D_{ci} L$	Nu	$0.023\ Re^{0.8}\mathrm{Pr}^{0.4}$
$\boldsymbol{A_{ri}}$	$\pi D_{ri} L$	h	$k\frac{Nu}{D_{ri}}$

The parameters and variables employed are listed in the nomenclature.

3.0 DETAILED PERFORMANCE ANALYSIS OF PTCS

The PTC thermal efficiency (η_{th}) and temperature difference $(\Delta T = T_{out} - T_{in})$ are defined as PFs. Thus, high η_{th} and ΔT indicate good thermal performance and low values indicate poor performance. Eight thermal fluids, i.e., four liquids (water, Therminol, molten salt, and liquid sodium) and four gases (air, carbon dioxide, helium, and hydrogen), are considered in the present analyses. The problem setup and the PTC geometry are performed in accordance with Table 2. Mass flow values of 2 $\frac{kg}{s}$ and 0.2 $\frac{kg}{s}$ are selected for the liquids and gases, respectively. The effect of inlet flow condition, reflector dimension, receiver diameter, and cover diameter on the PFs of the eight fluids is investigated by conducting 32 case studies.

Table 2. Problem setup and PTC geometry [2]

Parameter	Value	Parameter	Value
ϵ_r	0.095	L	12 m
ϵ_c	0.88	W	5.8 m
η_{opt}	0.9	f	1.71 m
G_b	800 $\frac{W}{m^2}$	T_{sun}	5770 K
T_{amp}	300 K	h_{out}	10 $\frac{W}{m^2K}$

Note that in all the following figures The solid line denotes the efficiency whereas the dashed line denoted the temperature difference.

4.0 RESULTS AND DISCUSSION

4.1 Effect of Inlet Flow Conditions

The effect of inlet flow condition is studied using level curves. Two variables are selected in the present analysis: the inlet flow temperature and the inlet mass flow rate. All other flow parameters are kept constant, as indicated in Table 2. The inlet temperature values employed are shown in Table 3.

Table 3. Range of inlet temperatures used in the present analyses

Liquids	T_{in} [K]	Gases	T_{in} [K]
Water	300 – 550	Air	300 – 1300
Therminol	300 – 580	Carbon dioxide	300 – 1300
Molten salt	550 – 800	Helium	300 – 1300
Liquid sodium	400 – 1100	Hydrogen	300 – 1100

Figure 2 and Figure 3 show the changes in the PFs with changing inlet temperature and mass flow rate. For all the liquids the mass flow rate changes from 0.1 to 2 $\frac{kg}{s}$ whereas for all the gases the flow rate changes from 0.05 to 0.2 $\frac{kg}{s}$. Regarding the thermal efficiency (η_{th}) of the fluids, the effect of inlet temperature is (in general) more significant than that of the mass flow rate. However, regarding ΔT, the effect of the flow rate is more significant than the effect of temperature. The temperature difference and thermal efficiency decrease (in general) with increasing inlet temperature, but this effect is more remarkable in the gases than fluids.

In the liquids (see Figure 2), the inlet temperature (in contrast to the mass flow rate) exerts more influence on the thermal efficiency than on the temperature difference. The mass flow rate exerts the least influence on the temperature difference associated with water. The temperature difference decreases with increasing mass flow rate and inlet temperature. Moreover, the thermal efficiency decreases with increasing inlet temperature.

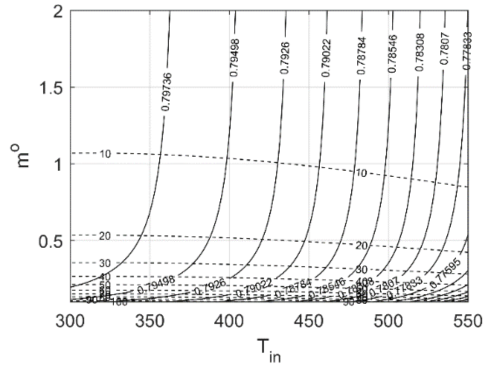

(a) Water

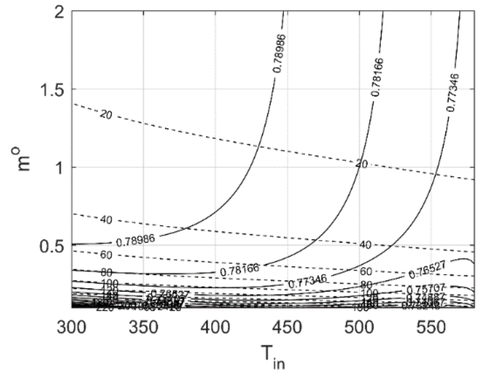

(b) Therminol

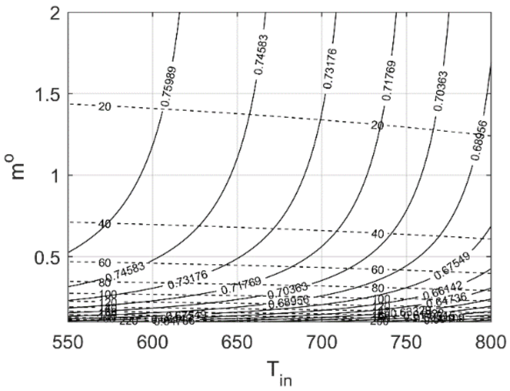

(c) Molten salt

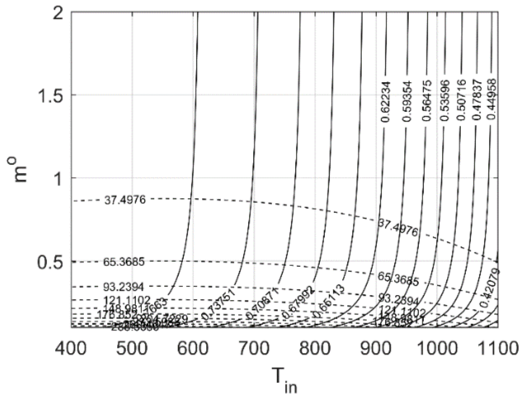

(d) Liquid sodium

Figure 2. Effect of inlet condition on liquid fluids

The inlet condition effect on the PFs is more significant for the gases than for the liquids (see Figure 3). Unlike the temperature difference values associate with the liquids, the values associate with the gases change considerably with both the inlet mass flow rate and inlet temperature. However, the PFs related to air and carbon dioxide change more significant than those related to helium and hydrogen. The temperature difference obtained for air and carbon dioxide is higher, but the maximum thermal efficiency is lower than those obtained for helium and hydrogen.

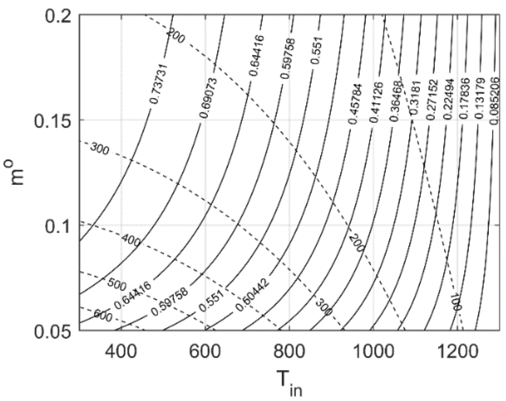

(a) Air

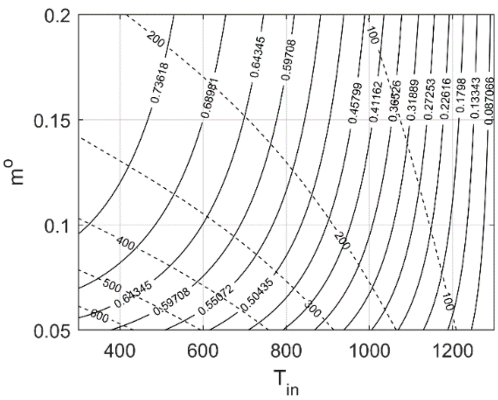

(b) Carbon dioxide

Figure 3. Effect of inlet condition on gas fluids

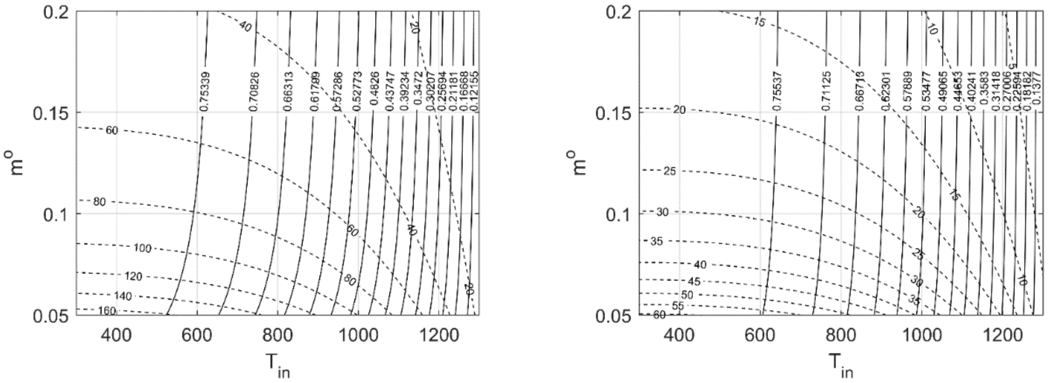

(c) Helium (d) Hydrogen

Figure 3. (cont.)

4.2 Effect of Reflector Geometry

The effect of the PTC length and width is assessed, and level curves are generated for the PFs, as shown in Figure and Figure . The reflector length and width are changed from 6 m to 24 m and from 2.9 m to 11.6 m, respectively. The inlet temperature is kept constant at 550 K, and the inlet mass flow rate is 2 $\frac{kg}{s}$ for liquids and 0.2 $\frac{kg}{s}$ for gases. All other parameters and variables are kept constant, as indicated in Table 2. The reflector geometry affects the temperature difference and thermal efficiency for both liquids and gases. However, the effect of the reflector length on the thermal efficiency is smaller than the effect of the reflector width, especially in the liquids. With changing reflector length, the thermal efficiency of the liquids remains nearly constant in case of water and Therminol (Figure), however it changes more notably in case of molten salt and liquid sodium.

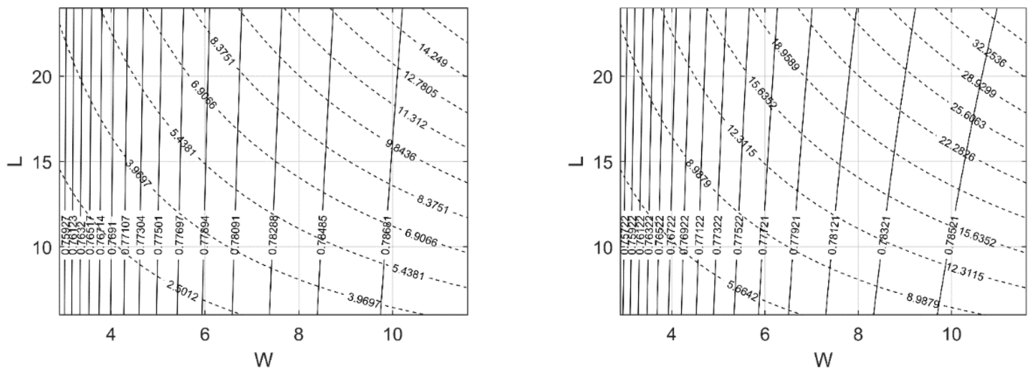

(a) Water (b) Therminol

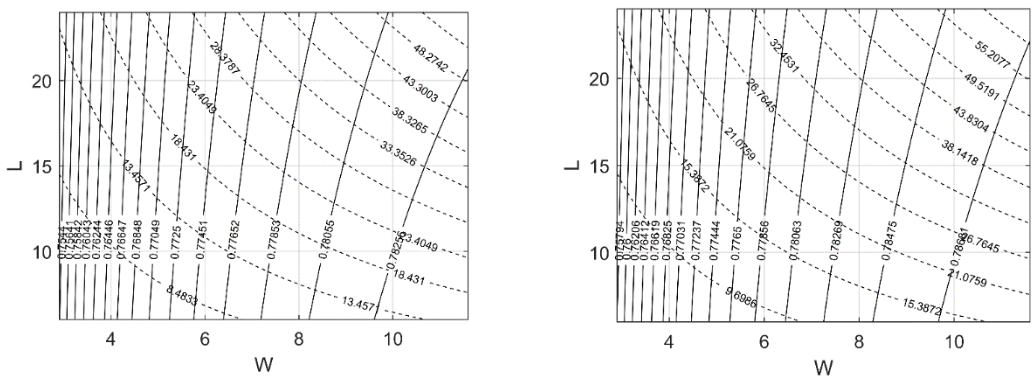

(c) Molten salt (d) Liquid sodium

Figure 4. Effect of reflector geometry on liquid fluids

In the gases (see Figure), the reflector geometry has a notable effect on the PFs. Compared with high values of the reflector width, low values of the width have a greater effect on the change in thermal efficiency, in air and carbon dioxide. The same temperature difference trend is observed for all three gases. However, the temperature difference values obtained for air and carbon dioxide are higher than those obtained for helium and hydrogen. The thermal efficiency behavior differs between these two pairs of gases. That is, with increasing reflector width, the thermal efficiency increases for helium and hydrogen, but changes only slightly for air and carbon.

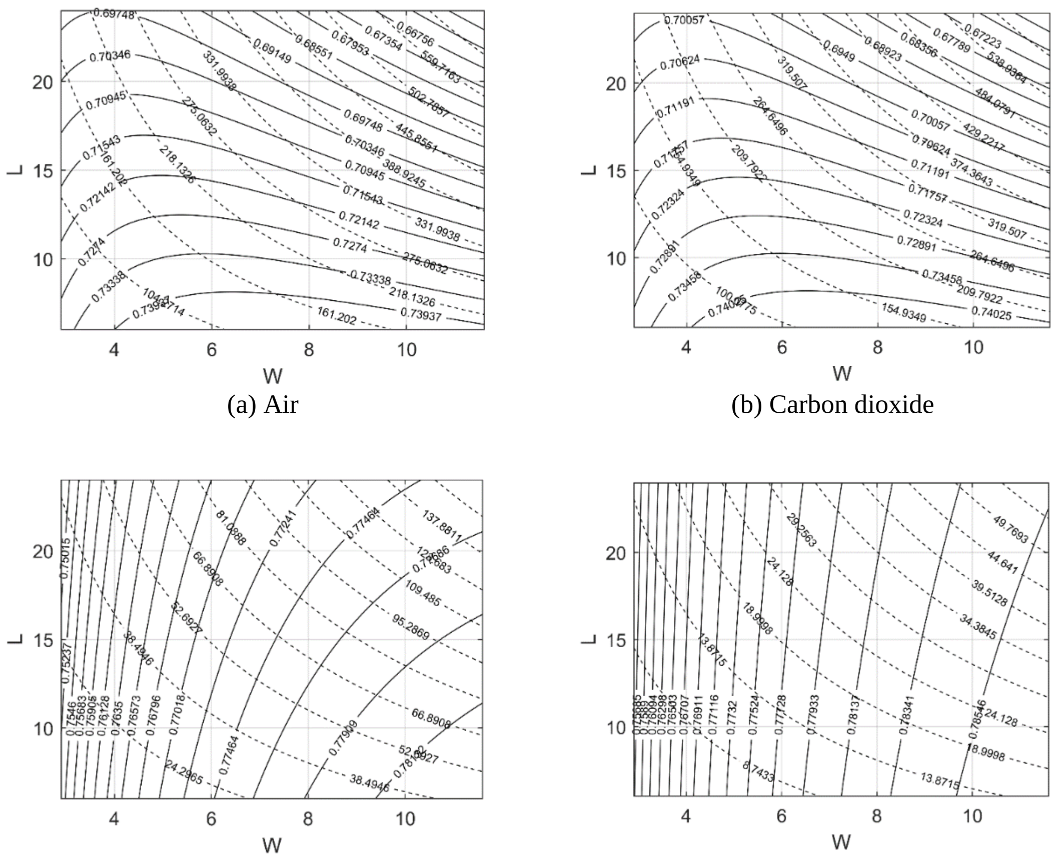

(a) Air (b) Carbon dioxide

(c) Helium (d) Hydrogen

Figure 5. Effect of reflector geometry on gas fluids

4.3 Effect of Receiver Diameter

The effect of the receiver inlet and outlet diameters is assessed, and level curves are generated for the performance factors as shown in Figure and Figure . The inlet diameter and the outlet diameter are changed from 0.01 m to 0.069 m and 0.07 m to 0.1 m, respectively. The inlet temperature is kept constant at 550 K, and the inlet mass flow rate is 2 $\frac{kg}{s}$ for liquids and 0.2 $\frac{kg}{s}$ for gases. All other parameters and variables are kept constant, as indicated in Table 2. The receiver diameter has a negligible effect on the temperature difference of each liquid and gas. However, the diameter has a significant effect on the thermal efficiency, especially in the case of the gases. For liquid sodium and water, the temperature difference and thermal efficiency remain nearly constant with changing inlet receiver diameter. Compared with the small effect observed for water, the effect of diameter is more significant in Therminol and molten salt.

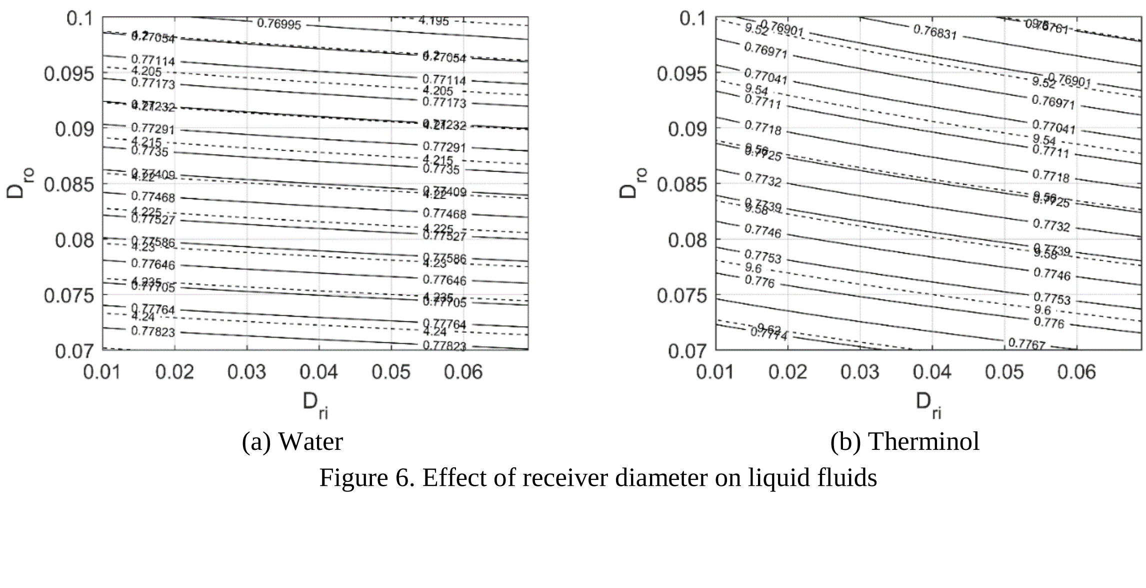

(a) Water (b) Therminol

Figure 6. Effect of receiver diameter on liquid fluids

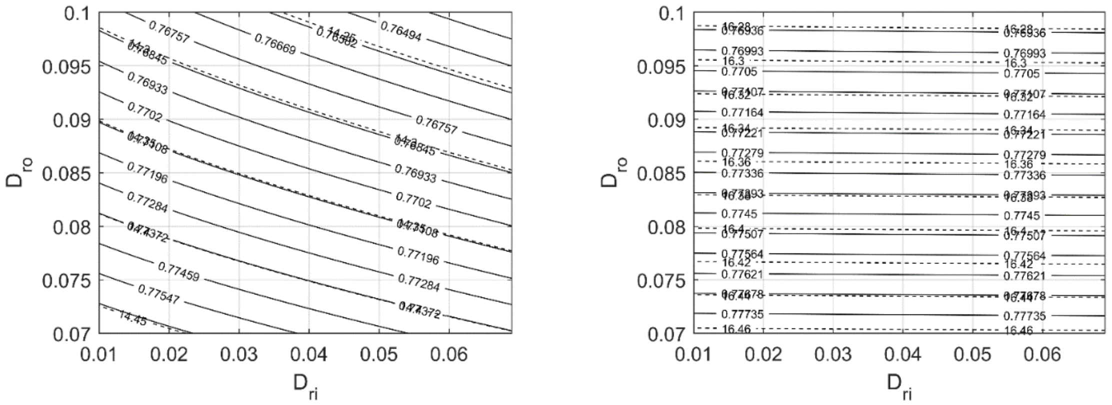

(c) Molten salt (d) Liquid sodium

Figure 6. (cont.)

In the gases (see Figure), the effect of both the inlet and outlet receiver diameters is clear. However, their effect in air and carbon dioxide is more notable than their effect in helium and hydrogen. The general trend observed for all the liquids and gases, is that the temperature difference and thermal efficiency both increase with increasing receiver outlet diameter.

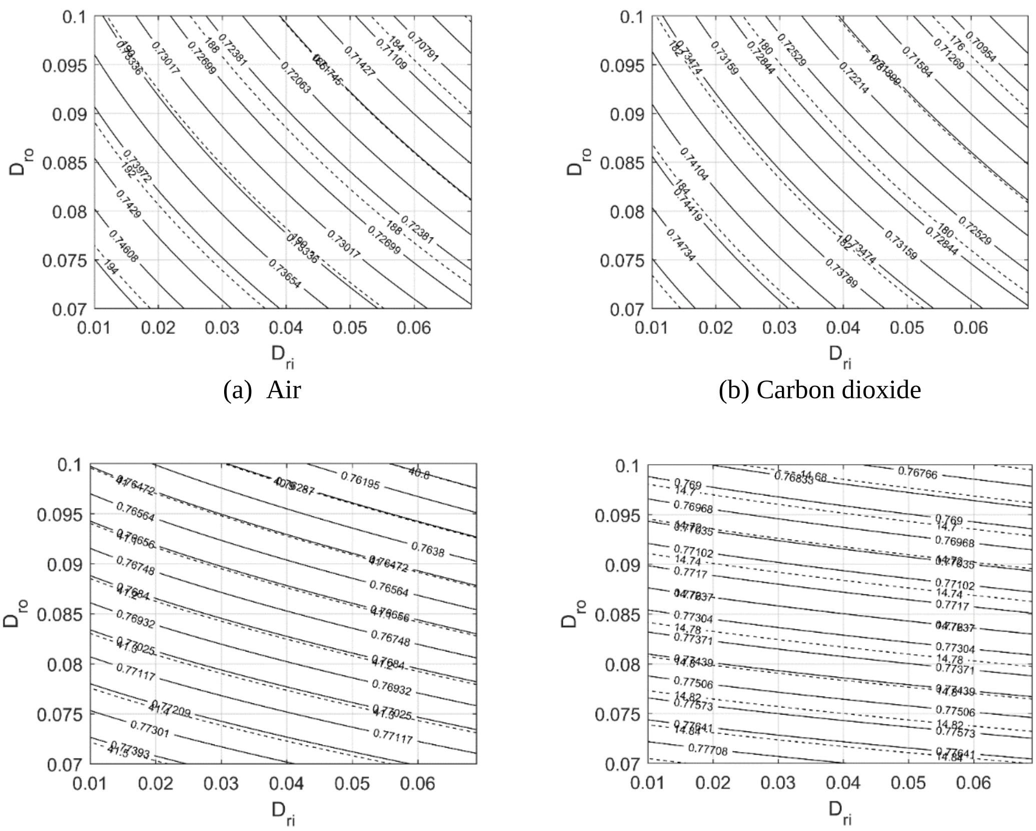

(a) Air (b) Carbon dioxide

(c) Helium (d) Hydrogen

Figure 7. Effect of receiver diameter on gas fluids

4.4 Effect of Cover Diameter

The effect of the cover inlet and outlet diameters is evaluated, and level curves are generated for the PFs, as shown in Figure and Figure . The inlet diameter and outlet diameter are changed from 0.08 m to 0.124 m and from 0.125 m to 0.2 m, respectively. The inlet temperature is kept constant at 550 K, and the inlet mass flow rate is 2 $\frac{kg}{s}$ for liquids and 0.2 $\frac{kg}{s}$ for gases. All other parameters and variables are kept constant (as indicated in Table 2). When the cover diameter is changed the change trends changes of the PFs associate with the liquids and gases are nearly the same. In addition, the effect of the diameter on the PFs is small compared with the effect of other geometric variables. All the liquids exhibit nearly the same thermal efficiency trend. However, the temperature difference values associate with molten salt and liquid sodium are higher than those obtained for water and Therminol.

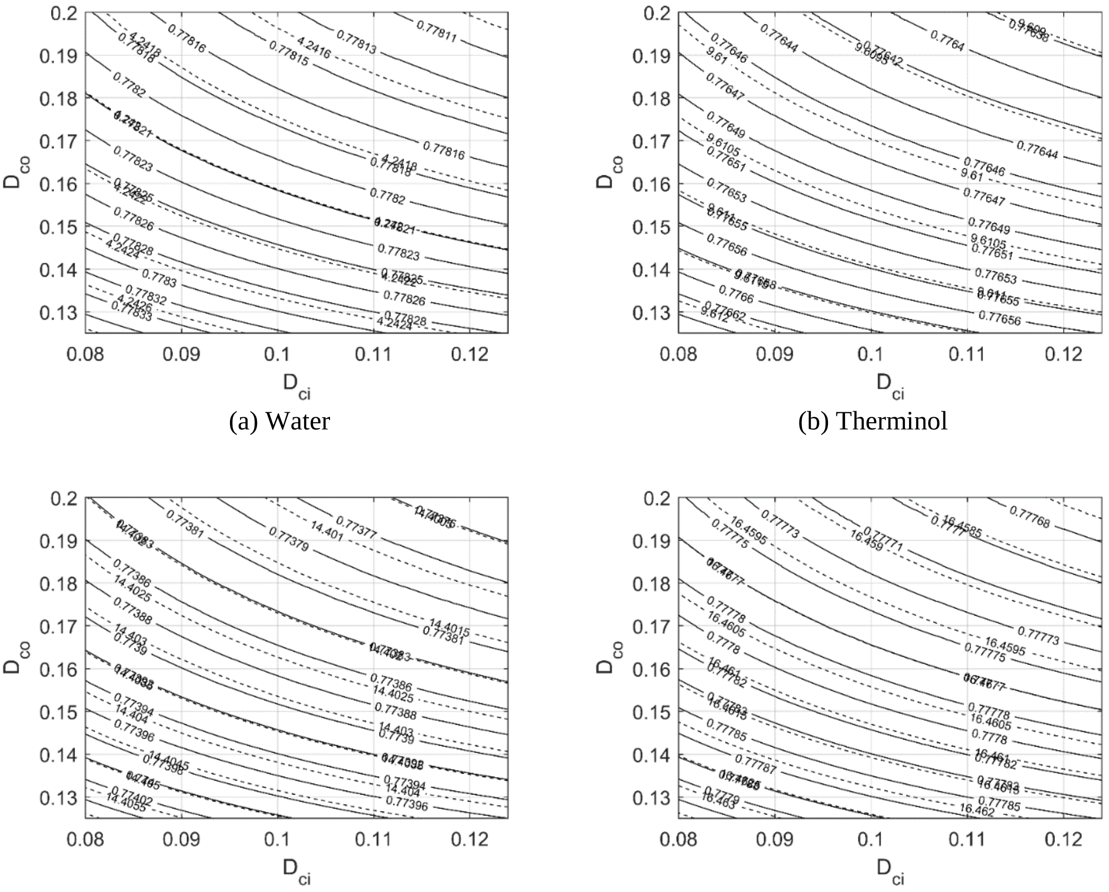

Figure 8. Effect of cover diameter on liquid fluids

The change in cover diameter has a minor effect on the PFs associate with the gases (Figure). The highest values of the temperature difference are obtained in the case of air and carbon dioxide, and the highest values of thermal efficiency are obtained in the case of helium and hydrogen. In general, for all liquids and gases, the temperature difference and thermal efficiency increase with increasing cover outlet diameter and decrease with increasing cover inlet diameter.

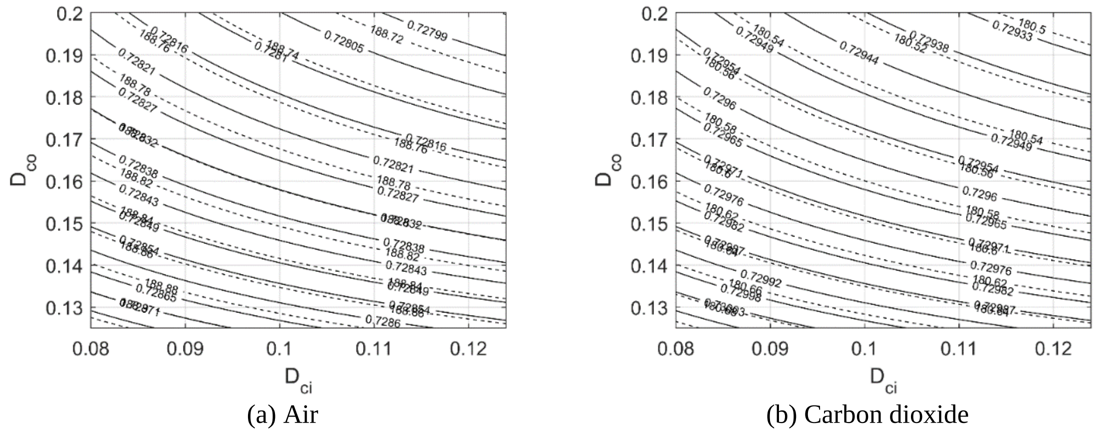

Figure 9. Effect of cover diameter on gas fluids

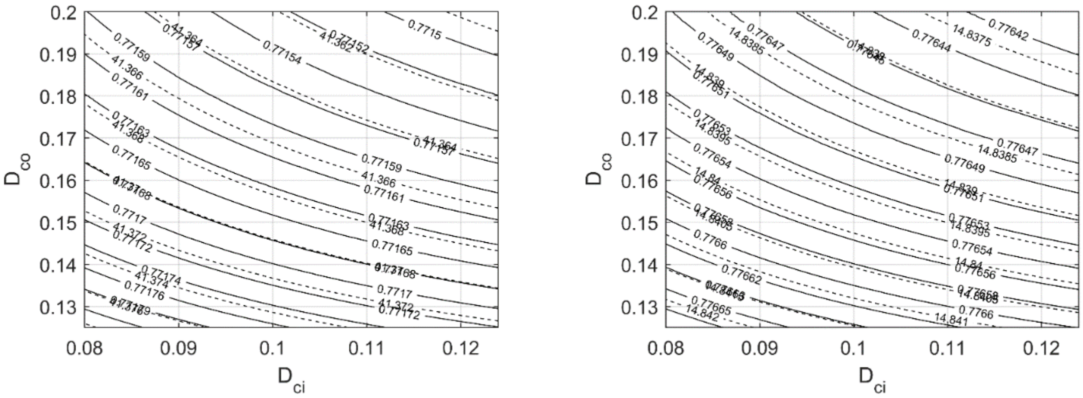

(c) Helium (d) Hydrogen

Figure 9. (cont.)

Table 4 summarizes the main findings of the present study. The first column Table 4lists the eight fluids used, and the second column lists the PFs (including the temperature difference and thermal efficiency). Furthermore, the last four columns list the maximum value of PF and the allowed range of change induced by each effect. In the present study, the maximum values of PFs and maximum ranges occur when the inlet conditions are changed; changes in the inlet temperature and changes in the reflector geometry yield the highest and second-highest values, respectively. The cover geometry has the minimum effect on the PFs. Moreover, the best maximum and the best maximum temperature difference are obtained for water and air, respectively. The maximum range of efficiency change is obtained for carbon dioxide.

The present results provide more inside and detailed performance analysis using eight working fluids in difference than any previous work which concentrated on selected number of working fluids each. The most relevant work that is related to the present study is the work of Bellos et al. [2] who study the performance of seven working fluids in response to the inlet temperature change without considering the effect of PTC geometry. However, both the present and previous works [2] considered the same benchmark problems, the present work can obtain a maximum thermal efficiency that is more than the previous efficiency. For the water as an example, the present maximum efficiency obtained is 79.97 %, where is the maximum efficiency based on [2] is 78.81 %. This improvement in thermal efficiency can be attributed to the change in PTC geometry in addition to the power of using the surface plots.

Table 4. Summary of the performance analysis findings

Fluid	PFs	Inlet conditions		Reflector geometry		Receiver geometry		Cover geometry	
		Maximum	Range	Maximum	Range	Maximum	Range	Maximum	Range
Water	ΔT [K]	106.16	101.92	17.19	16.15	4.25	0.0516	4.24	0.0015
	η_{th} %	79.97	3.8	78.88	3.15	77.88	0.95	77.84	0.027
Therminol	ΔT [K]	235.75	226.54	38.9	36.56	9.63	0.14	9.61	0.004
	η_{th} %	79.81	13.12	78.72	3.2	77.81	1.12	77.67	0.029
Molten salt	ΔT	242.85	230.35	58.22	54.71	14.47	0.26	14.41	0.006
	η_{th}	77.4	22.51	78.46	3.22	77.72	1.4	77.41	0.0322
Liquid sodium	ΔT	316.2	306.57	66.59	62.58	16.46	0.19	16.46	0.0058
	η_{th}	79.51	46.07	78.89	3.3	77.79	0.91	77.79	0.0273
Air	ΔT	684.89	668.4	673.58	626.24	195.05	13.19	188.93	0.23
	η_{th}	78.39	74.53	74.54	9.57	75.24	5.09	72.88	0.0885
Carbon dioxide	ΔT	684.26	668.79	648.65	603.43	186.52	12.47	180.71	0.215
	η_{th}	78.25	74.18	74.59	9.07	75.36	5.04	73.01	0.087
Helium	ΔT	169.73	164.61	166.28	156.18	41.54	0.79	41.38	0.0188
	η_{th}	79.85	72.21	78.35	3.56	77.49	1.47	77.18	0.035
Hydrogen	ΔT	60.72	52.78	60.026	56.41	14.86	0.206	14.84	0.0055
	η_{th}	79.95	39.1	78.75	3.27	77.78	1.08	77.67	0.029

5.0 CONCLUSIONS

In the present work, the performance of parabolic trough collectors is analyzed. The effect of their geometry and inlet conditions on selected performance factors (PFs) is studied using surface plots. Eight thermal working fluids are included in the present analyses: four liquids (water, Therminol, molten salt, and liquid sodium) and four gases (air, carbon dioxide, helium, and hydrogen). Four effects are investigated, i.e. the effect of (1) inlet mass flow rate and inlet temperature (m^o and T_{in}), (2) reflector geometric length and width (L and W), (3) receiver inlet and outlet diameters (D_{ri} and D_{ro}), and cover inlet and outlet diameters (D_{ci} and D_{co}).

The performance parameters are defined as the thermal efficiency and temperature difference between inlet and outlet. Subsequently, high values of performance factors indicate good PTC thermal performance. The effect of inlet conditions is investigated in terms of the inlet temperature and mass flow rate. the effect of inlet temperature is more significant than the mass flow rate effect on the thermal efficiency, whereas this effect is reversed in case of the temperature difference, by which the mass flow rate exerts the least influence on the temperature difference. Regarding the geometric parameters, the effect of the reflector length on the thermal efficiency is smaller than the effect of the reflector width. Both the receiver and cover diameters a negligible effect in comparison to the other studied parameters. These important findings can help in the design and selection of PTC design variables and parameters. A more development is recommended for future work in both the mathematical models and parametric study to much improve the PTCs performance.

It is worth to note that the present models do not consider the phase change of the fluids and can only be applied within the working fluid temperatures. The present model also assumes steady state conditions. It is recommenced for future work to enhance the present model to consider both the phase change and time dependence.

6.0 ACKNOWLEDGEMENT

There is no acknowledgement related to the present work.

7.0 NOMENCLATURE

A_a	Aperture area	T_{sun}	Sun temperature
A_{co}	Cover inlet area	T_{am}	Ambient temperature
A_{ci}	Cover inlet area	T_{in}	Inlet temperature
A_{ro}	Receiver outlet area	T_{out}	Outlet temperature
A_{ri}	Receiver inlet area	W	Reflector width
C_p	Specific heat coefficient at constant pressure	ϵ_r	Emissivity of receiver tube
f	Reflector radius	ϵ_c	Emissivity of glass tube
G_b	Solar beam irradiation	η_{opt}	Optical efficiency
H_{out}	Outlet convection coefficient	μ	Dynamic viscosity
L	Tube length	σ	Stefan-Boltzman constant
m^o	Mass flow rate	ρ	Density
k	Thermal conductivity		

8.0 REFERENCES

[1] H. Price *et al.*, “Advances in parabolic trough solar power technology,” *Journal of Solar Energy Engineering*, vol. 124, no. 2, pp. 109–125, 2002.

[2] E. Bellos, C. Tzivanidis, and K. A. Antonopoulos, “A detailed working fluid investigation for solar parabolic trough collectors,” *Applied Thermal Engineering*, vol. 114, pp. 374–386, 2017.

[3] A. Malan and K. Ravi Kumar, “A comprehensive review on optical analysis of parabolic trough solar collector,” *Sustainable Energy Technologies and Assessments*, vol. 46, p. 101305, 2021.

[4] M. M. Ibrahim and M. M. Kasem, “Numerical thermal study of heat transfer enhanced in laminar-turbulent transition flow through absorber pipe of parabolic solar trough collector system,” *Frontiers in Heat and Mass Transfer*, vol. 17, pp. 1-11, 2021.

[5] W. Fuqiang, C. Ziming, T. Jianyu, Y. Yuan, S. Yong, and L. Linhua, “Progress in concentrated solar power technology with parabolic trough collector system: A comprehensive review,” *Renewable and Sustainable Energy Reviews*, vol. 79, pp. 1314–1328, 2017.

[6] S. Raja Narayanan and S. Vijay, “Desalination of water using parabolic trough collector,” *Materials Today: Proceedings*, vol. 21, pp. 375–379, 2020.

[7] L. S. Mendoza Castellanos, A. L. Galindo Noguera, E. I. Gutiérrez Velásquez, G. E. C. Caballero, E. E. Silva Lora, and V. R. Melian Cobas, “Mathematical modeling of a system composed of parabolic trough solar collectors integrated with a hydraulic energy storage system,” *Energy*, vol. 208, p. 118255, 2020.

[8] M. A. Haghghi, Z. Mohammadi, S. M. Pesteei, A. Chitsaz, and K. Parham, “Exergoeconomic evaluation of a system driven by parabolic trough solar collectors for combined cooling, heating, and power generation; A case study,” *Energy*, vol. 192, p. 116594, 2020.

[9] Y. Bi, L. Qin, J. Guo, H. Li, and G. Zang, "Performance analysis of solar air conditioning system based on the independent-developed solar parabolic trough collector," *Energy*, vol. 196, p. 117075, 2020.

[10] P. K. Ktistis, R. A. Agathokleous, and S. A. Kalogirou, "Experimental performance of a parabolic trough collector system for an industrial process heat application," *Energy*, vol. 215, p. 119288, 2021.

[11] İ. H. Yılmaz and A. Mwesigye, "Modeling, simulation and performance analysis of parabolic trough solar collectors: A comprehensive review," *Applied Energy*, vol. 225, pp. 135–174, 2018.

[12] B. Zou, Y. Jiang, Y. Yao, and H. Yang, "Impacts of non-ideal optical factors on the performance of parabolic trough solar collectors," *Energy*, vol. 183, pp. 1150–1165, 2019.

[13] S. A. Kalogirou, "A detailed thermal model of a parabolic trough collector receiver," *Energy*, vol. 48, no. 1, pp. 298–306, 2012.

[14] T. Fasquelle, Q. Falcoz, P. Neveu, F. Lecat, and G. Flamant, "A thermal model to predict the dynamic performances of parabolic trough lines," *Energy*, vol. 141, pp. 1187–1203, 2017.

[15] M. M. Heyhat, M. Valizade, Sh. Abdolahzade, and M. Maerefat, "Thermal efficiency enhancement of direct absorption parabolic trough solar collector (DAPTSC) by using Nanofluid and metal foam," *Energy*, vol. 192, p. 116662, 2020.

[16] D. Lei, X. Fu, Y. Ren, F. Yao, and Z. Wang, "Temperature and thermal stress analysis of parabolic trough receivers," *Renewable Energy*, vol. 136, pp. 403–413, 2019.

[17] R. V. Padilla, G. Demirkaya, D. Y. Goswami, E. Stefanakos, and M. M. Rahman, "Heat transfer analysis of parabolic trough solar receiver," *Applied Energy*, vol. 88, no. 12, pp. 5097–5110, 2011.

[18] J. Jin, Y. Ling, and Y. Hao, "Similarity analysis of parabolic-trough solar collectors," *Applied Energy*, vol. 204, pp. 958–965, 2017.

[19] B. Zou, Y. Yao, Y. Jiang, and H. Yang, "A new algorithm for obtaining the critical tube diameter and intercept factor of parabolic trough solar collectors," *Energy*, vol. 150, pp. 451–467, 2018.

[20] G. A. Salazar, N. Fraidenraich, C. A. A. de Oliveira, O. de Castro Vilela, M. Hongn, and J. M. Gordon, "Analytic modeling of parabolic trough solar thermal power plants," *Energy*, vol. 138, pp. 1148–1156, 2017.

[21] H. Liang, S. You, and H. Zhang, "Comparison of different heat transfer models for parabolic trough solar collectors," *Applied Energy*, vol. 148, pp. 105–114, 2015.

[22] M. Fan, H. Liang, S. You, H. Zhang, W. Zheng, and J. Xia, "Heat transfer analysis of a new volumetric based receiver for parabolic trough solar collector," *Energy*, vol. 142, pp. 920–931, 2018.

[23] A. Yadav and M. Kumar, "Experimental study and analysis of parabolic trough collector with various reflectors," *International Journal of Energy and Power Engineering*, vol. 7, no. 12, p. 5, 2013.

[24] S. M. Sadegh Hosseini and M. S. Dehaj, "An experimental study on energetic performance evaluation of a parabolic trough solar collector operating with Al_2O_3/water and GO/water Nanofluids," *Energy*, vol. 234, p. 121317, 2021.

[25] Z. D. Cheng, Y. L. He, F. Q. Cui, B. C. Du, Z. J. Zheng, and Y. Xu, "Comparative and sensitive analysis for parabolic trough solar collectors with a detailed Monte Carlo ray-tracing optical model," *Applied Energy*, vol. 115, pp. 559–572, 2014.

[26] W. Yuanjing, Z. Cheng, Z. Yanping, and H. Xiaohong, "Performance analysis of an improved 30 MW parabolic trough solar thermal power plant," *Energy*, vol. 213, p. 118862, 2020.

[27] R. V. Padilla, A. Fontalvo, G. Demirkaya, A. Martinez, and A. G. Quiroga, "Exergy analysis of parabolic trough solar receiver," *Applied Thermal Engineering*, vol. 67, no. 1–2, pp. 579–586, 2014.

[28] J. D. Osorio and A. Rivera-Alvarez, "Performance analysis of parabolic trough collectors with double glass envelope," *Renewable Energy*, vol. 130, pp. 1092–1107, 2019.

[29] A. A. Ghoneim and A. M. Mohammedein, "Parabolic trough collector performance in a hot climate," *Journal of Energy Engineering*, vol. 142, no. 1, p. 04015008, 2016.

[30] H. Yang, Q. Wang, J. Cao, G. Pei, and J. Li, "Potential of performance improvement of concentrated solar power plants by optimizing the parabolic trough receiver," *Frontier in Energy*, vol. 14, no. 4, pp. 867–881, 2020.

[31] M. M. Kasem, "Multiobjective design optimization of parabolic trough collectors," *Scientific Reports*, vol. 12, p. 19964, 2022.